

Peripheral Lesions Identified by Mydriatic Ultrawide Field Imaging: Distribution and Potential Impact on Diabetic Retinopathy Severity

Paolo S. Silva, MD,^{1,2} Jerry D. Cavallerano, OD, PhD,^{1,2} Jennifer K. Sun, MD, MPH,^{1,2}
Ahmed Z. Soliman, MD,^{1,2} Lloyd M. Aiello, MD,^{1,2} Lloyd Paul Aiello, MD, PhD^{1,2}

Objective: To assess diabetic retinopathy (DR) as determined by lesions identified using mydriatic ultrawide field imaging (DiSLO200; Optos plc, Scotland, UK) compared with Early Treatment Diabetic Retinopathy Study (ETDRS) 7-standard field film photography.

Design: Prospective comparative study of DiSLO200, ETDRS 7-standard field film photographs, and dilated fundus examination (DFE).

Participants: A total of 206 eyes of 103 diabetic patients selected to represent all levels of DR.

Methods: Subjects had DiSLO200, ETDRS 7-standard field film photographs, and DFE. Images were graded for severity and distribution of DR lesions. Discrepancies were adjudicated, and images were compared side by side.

Main Outcome Measures: Distribution of hemorrhage and/or microaneurysm (H/Ma), venous beading (VB), intraretinal microvascular abnormality (IRMA), and new vessels elsewhere (NVE). Kappa (κ) and weighted κ statistics for agreement.

Results: The distribution of DR severity by ETDRS 7-standard field film photographs was no DR 12.5%; nonproliferative DR mild 22.5%, moderate 30%, and severe/very severe 8%; and proliferative DR 27%. Diabetic retinopathy severity between DiSLO200 and ETDRS film photographs matched in 80% of eyes (weighted $\kappa = 0.74, \kappa = 0.84$) and was within 1 level in 94.5% of eyes. DiSLO200 and DFE matched in 58.8% of eyes (weighted $\kappa = 0.69, \kappa = 0.47$) and were within 1 level in 91.2% of eyes. Forty eyes (20%) had DR severity discrepancies between DiSLO200 and ETDRS film photographs. The retinal lesions causing discrepancies were H/Ma 52%, IRMA 26%, NVE 17%, and VB 4%. Approximately one-third of H/Ma, IRMA, and NVE were predominantly outside ETDRS fields. Lesions identified on DiSLO200 but not ETDRS film photographs suggested a more severe DR level in 10% of eyes. Distribution in the temporal, superotemporal, inferotemporal, superonasal, and inferonasal fields was 77%, 72%, 61%, 65%, and 59% for H/Ma, respectively ($P < 0.0001$); 22%, 24%, 21%, 28%, and 22% for VB, respectively ($P = 0.009$); 52%, 40%, 29%, 47%, and 36% for IRMA, respectively ($P < 0.0001$), and 8%, 4%, 4%, 8%, and 5% for NVE, respectively ($P = 0.03$). All lesions were more frequent in the temporal fields compared with the nasal fields ($P < 0.0001$).

Conclusions: DiSLO200 images had substantial agreement with ETDRS film photographs and DFE in determining DR severity. On the basis of DiSLO200 images, significant nonuniform distribution of DR lesions was evident across the retina. The additional peripheral lesions identified by DiSLO200 in this cohort suggested a more severe assessment of DR in 10% of eyes than was suggested by the lesions within the ETDRS fields. However, the implications of peripheral lesions on DR progression within a specific ETDRS severity level over time are unknown and need to be evaluated prospectively.

Financial Disclosure(s): Proprietary or commercial disclosure may be found after the references. *Ophthalmology* 2013;120:2587–2595 © 2013 by the American Academy of Ophthalmology.



Management of diabetic eye disease is guided by landmark clinical trials conducted during the past 40 years.^{1–10} These clinical trials established treatment modalities and elucidated the risk for progression, visual loss, and response to treatment on the basis of the severity level of diabetic retinopathy (DR). In these trials, DR was evaluated using

mydriatic stereoscopic 30-degree 35-mm retinal photography obtained using a defined protocol of 7-standard retinal fields in what is referred to as “Early Treatment Diabetic Retinopathy Study (ETDRS) protocol fundus photography.” This method of retinal evaluation has been widely adopted and has generally remained the gold standard for evaluation

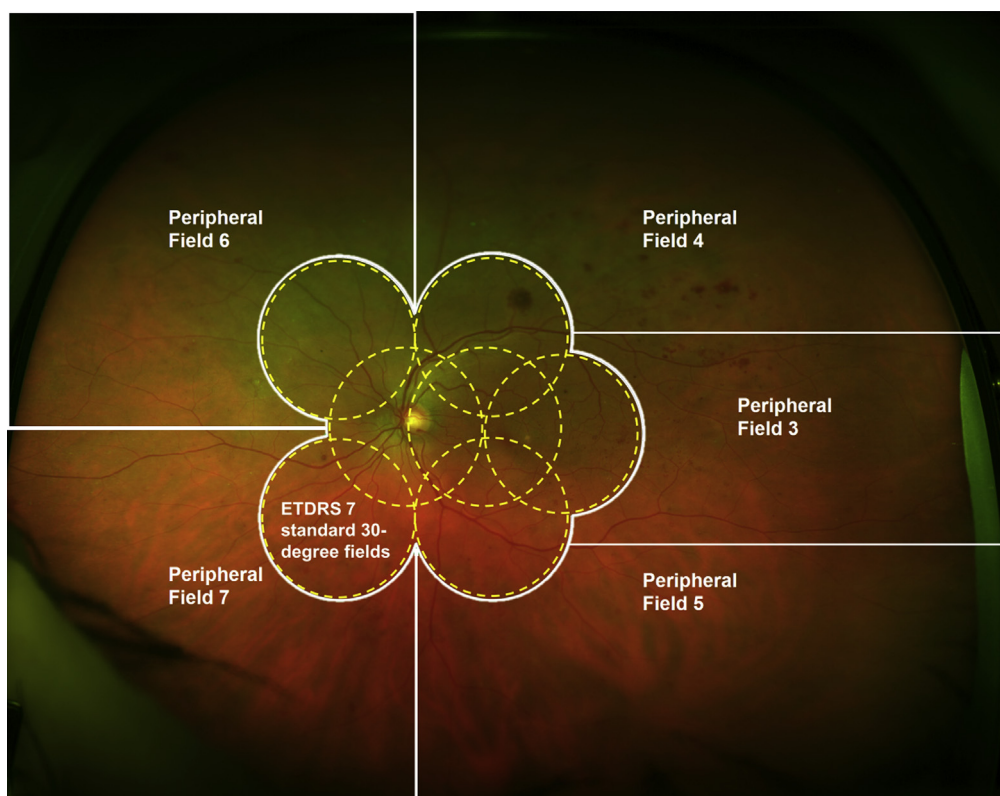


Figure 1. A mydriatic ultrawide field 200-degree image with overlay of the Early Treatment Diabetic Retinopathy Study (ETDRS) 7-standard 30-degree fields and the ultrawide peripheral fields used in this study.

of DR in both clinical and research settings. The technique recently has moved from film to digital imaging, otherwise using essentially the same imaging technique and maintaining comparable agreement.^{11–13}

The ETDRS film photography protocol covers approximately the central posterior 90 degrees of the retina, representing only approximately 30% of the entire retinal surface area (Fig 1). The assessment of DR severity using ETDRS film photographs relies only on retinal lesions located within this posterior area of the retina and does not account for or define criteria for retinal lesions that may be present in the retinal periphery outside the imaged area. Nevertheless, DR severity determined using ETDRS film photographs closely identifies the risk of retinopathy progression and visual loss.⁴

Retinal imaging technology has advanced greatly since the initiation of the film photographs protocol. For example, imaging with the Optos P200MA (Optos plc, Scotland, UK) now allows ultrawide field evaluation that visualizes extensive areas of contiguous retinal periphery. Rather than imaging 30 degrees of retina at a time (~5% of the retinal area) as with ETDRS film photographs, the Optos system images up to 200 degrees in a single image, representing approximately 82% of the retinal area, with a resolution of 14 μm and an acquisition time of 0.25 seconds. This imaging is accomplished using scanning laser ophthalmoscope technology combined with the unique optical properties of an ellipsoidal mirror. The comparison between nonmydriatic ultrawide field images and ETDRS

film photographs and dilated fundus examination (DFE) has been reported and has demonstrated substantial agreement with ETDRS film photographs (kappa = 0.79 [95% confidence interval {CI}, 0.73–0.86], weighted kappa = 0.85 [95% CI, 0.80–0.91]) and DFE (kappa = 0.61 [95% CI, 0.53–0.69], weighted kappa = 0.77 [95% CI, 0.71–0.84]).¹⁴

Ultrawide field 200-degree images cover substantial areas of retina traditionally not visualized by the ETDRS 7-standard fields, allowing the simultaneous evaluation of both the posterior pole and the retinal periphery in a single image. As a result, accurate characterization of the presence and distribution of DR lesions across nearly the entire retina is possible. The importance of identifying DR lesions outside the coverage of ETDRS 7-standard fields and assessing whether this identification adds substantially to determining DR severity level has not been fully evaluated.

Several limitations of nonmydriatic ultrawide field imaging exist. Ultrawide field images may have inherent distortion and color variation due to the required optics and scanning laser light source. In addition, a single ultrawide field may contain both sharply focused and less sharply focused areas resulting from spherical aberration of the ellipsoidal mirror and the spherical curvature of the eye over such large surface areas. These limitations observed under nonmydriatic conditions^{14–16} might be mitigated with mydriatic image capture with its increased retinal illumination and increased depth of focus for a given resolution and field of view.

In this study we obtained mydriatic ultrawide field fundus images using the Optos P200MA imaging system (DiSLO200) and compared lesion identification and location both within and outside the retinal area covered by ETDRS protocol 7-standard field imaging performed at the same visit. Evaluation included the frequency, type, severity, and location of DR lesions not observed by ETDRS 7-standard field imaging or DFE. We also compared mydriatic and nonmydriatic ultrawide field image quality and lesion detection capabilities.

Methods

A single-site, prospective, clinic-based, comparative instrument validation study evaluated agreement among nonmydriatic 100/200-degree images (Optomap; Optos plc), mydriatic 200-degree images (DiSLO200), DFE, and stereoscopic ETDRS 7-field 35-mm color film slides in determining DR severity. The retinal distribution of DR lesions and the agreement of DiSLO200 for DR severity with ETDRS film photographs and DFE were determined. The study design was consistent with the tenets of the Declaration of Helsinki, and the Committee on Human Studies of the Joslin Diabetes Center approved all procedures. Informed consent was obtained from all patients before study participation, and the conduct of the study complied with the Health Insurance Portability and Accountability Act.

Patient eligibility was determined from medical record review of the most recently diagnosed clinical level of DR severity. Study participants were selected to ensure distribution of various severity levels of DR, ranging from no DR to high-risk proliferative DR (PDR). Patients were eligible for the study if they met all the following inclusion criteria: age ≥ 18 years, diagnosis of type 1 or 2 diabetes mellitus as defined by the American Diabetes Association, willingness to sit through photography and imaging sessions, and willingness to sign the institutionally approved informed consent specifically designed for this study. Patients were excluded from the study if they had no history of diabetes, had a history of a condition in either eye that might preclude pupil dilation, were using eye drops (mydriatic or miotic) that would alter pupil size or reactivity, or had media opacities precluding adequate imaging of the retina.

DiSLO200 images, ETDRS film photographs, and DFE by retina specialist masked to the imaging were performed on 102 of the 103 enrolled patients at a single clinical visit. One enrolled patient subsequently refused dilation. Mydriasis was achieved with topical instillation of 2.5% phenylephrine hydrochloride and 1.0% tropicamide. All DFEs were performed by Beetham Eye Institute retinal specialists during the same patient visit and entered into standardized templates for ETDRS grading of DR severity on the electronic medical record. Retinal images were graded by a separate retinal specialist masked to the findings of the dilated fundus examination.

Stereoscopic 7-field ETDRS 35-mm color film slides were evaluated on a standard slide light box through Donaldson viewers according to ETDRS protocol by a retina specialist (P.S.S.) experienced in grading DR. Retinal findings were recorded directly onto a standardized electronic template modified from the Wisconsin Reading Center ETDRS retinal evaluation form and using unique patient study identification numbers. Grading was performed on the basis of the ETDRS protocol to determine the presence and severity of the following lesions: hemorrhage and/or microaneurysm (H/Ma), intraretinal microvascular abnormality (IRMA), venous beading (VB), cotton wool spots, hard exudate (HE), retinal thickening, new vessels on the disc (NVD), new vessels elsewhere (NVE) on the retina, pre-retinal hemorrhage, vitreous hemorrhage, and traction retinal detachment.

The same retinal specialist graded DiSLO200 images more than 2 years after evaluation of the original ETDRS film photographs, which also had been graded in a masked manner. All previous retinal findings were masked and unknown at the time the DiSLO200 images were evaluated. The same template used for recording findings from ETDRS film photographs was used to record the retinal findings in the DiSLO200 images. The method by which the ultrawide field images were evaluated has been described.¹⁴ Briefly, this grading required that the grader record the presence and degree of the same lesions as done for ETDRS 7-standard fields. The recording template was a modification of the template used for recording findings from ETDRS 7-standard fields. To grade the DiSLO200 images with respect to ETDRS 7-standard 30-degree fields, the grader defined field 1 as centered on the optic disc and including the retinal area bounded by a radius defined as the distance between the center of the optic disc to the fovea, field 2 as centered on the fovea and including the retinal area bounded by a radius defined as the distance between the fovea and the center of the optic disc, and field 3 as the area of the retina temporal to the fovea. The superior and inferior limits of field 3 were defined by imaginary horizontal lines at the uppermost and lowermost positions of the superior and inferior temporal vascular arcades, respectively. Imaginary vertical and horizontal lines through the center of the optic disc defined fields 4 (superior temporal), 5 (inferior temporal), 6 (superior nasal), and 7 (inferior nasal).

Nonsimultaneous stereoscopic ultrawide field images were acquired by capturing sequential images approximately 2 to 5 degrees apart. The ultrawide field images were viewed as uncompressed files. Screen-Vu stereoscope viewers (PS Mfg., Portland, OR) were used to achieve stereoscopic viewing. Images were viewed stereoscopically with each image of the stereoscopic pair displayed separately on Dell UltraSharp 2007FP 20-inch flat panel LCD monitors (Dell Inc, Round Rock, TX) with 1200 \times 1600 pixel resolution in 32-bit color with a Radeon 9250 video card (Advanced Micro Devices Inc, Sunnyvale, CA) as part of a 4-monitor reading station. The monitors used were part of the centralized reading center of the Joslin Vision Network and had been calibrated to a color temperature of 6500K and a gamma setting of 2.2 (i1Display, Greytac Macbeth; X-Rite Inc, Grand Rapids, MI). The readers had the ability to magnify and adjust the image color, contrast, brightness, and gamma correction. Each color composite ultrawide field image had a resolution of 3074 \times 3073 pixels covering approximately 200 degrees of retinal area. A senior retina specialist (L.P.A.), masked to previous gradings, adjudicated all DR severity discrepancies. All images with remaining DR severity discrepancies underwent a side-by-side comparison to identify the reason for the discrepancy and determine the apparently more accurate imaging modality.

To assess the retinal distribution of DR lesions in DiSLO200 images, peripheral fields were defined on the basis of an extension of ETDRS-defined standard fields and designated peripheral fields 3 to 7 (Fig 1). Field 3 as defined by the ETDRS is temporal to the macula with the nasal edge bisecting the macula. Peripheral field 3 encompasses the retinal area outside ETDRS field 3 and extends peripherally bordered superiorly and inferiorly by imaginary horizontal lines at the uppermost and lowermost positions of the superior and inferior temporal vascular arcades. Likewise, peripheral fields 4 to 7 were defined as peripheral retinal areas on DiSLO200 images not covered by corresponding ETDRS fields 4 to 7. An imaginary vertical line through the center of the optic disc delineated the temporal and nasal fields, a horizontal line bisecting the optic disc delineated the superior and inferior nasal fields, and the superior and inferior arcades delineated the superior and inferior temporal fields. Figure 1

overlays the ETDRS field template with the DiSLO200 peripheral fields.

The distribution of H/Ma, VB, IRMA, and NVE on DiSLO200 imaging was compared with the standard ETDRS photograph template, and the distribution of each lesion was characterized as follows: (1) lesion predominantly or only present within ETDRS fields, (2) lesion predominantly or only present outside ETDRS fields, (3) lesion distributed approximately equally in areas imaged and not imaged by ETDRS fields, (4) ETDRS field not gradable, and (5) peripheral DiSLO200 field not gradable.

Statistical Analysis

Clinical ETDRS levels of DR severity identified on ultrawide field images and ETDRS film photographs were cross-tabulated, and agreement between these results was assessed by calculating both unweighted kappa (κ) and weighted (using a linear scheme) κ values. Images that were classified as ungradable were excluded from the analysis. Landis and Koch¹⁷ guidelines for interpretation of κ and weighted κ statistics were used: 0.0 to 0.2 = slight agreement, 0.21 to 0.40 = fair agreement, 0.41 to 0.60 = moderate agreement, 0.61 to 0.80 = substantial agreement, and 0.81 to 1.00 = almost perfect agreement.¹⁸ Agreement between gradings for both overall severity of DR level and presence and extent of individual lesions was also assessed by calculating sensitivity/specificity percentages and positive/negative predictive values. The analysis of the distribution of DR lesions was only performed in retinal fields where the DR lesion evaluated was present and both ETDRS film photographs and DiSLO200 images were gradable. Chi-square analysis was performed to compare the distribution of DR lesions among the different fields. Results were not adjusted for correlations between retinopathy level data from eyes within the same subject. All statistical analyses were performed using SAS version 9.2 (SAS Inc, Cary, NC).

Results

A total of 206 eyes of 103 patients with type 1 or 2 diabetes were enrolled in this study. Mydriatic ultrawide field imaging was performed and completed in 204 eyes (99%) (1 patient [2 eyes] refused imaging). Complete ETDRS film photographs were available in 200 eyes (97.1%) (1 patient [2 eyes] refused imaging with film, and in 4 eyes of 4 different patients the film did not advance in the camera or the 35-mm slides were not returned from the processing laboratory). Table 1 shows the subject characteristics and visual acuity at enrollment and the distribution of DR and DME severity as graded by ETDRS film photographs. The agreement between 2 sets (mydriatic and nonmydriatic) of 200-degree ultrawide field images taken of the same patient at the same patient visit evaluated by 2 readers masked to results had an unweighted κ agreement of 0.62 ± 0.04 (95% CI, 0.54–0.70) and weighted κ of 0.79 ± 0.03 (95% CI, 0.74–0.85).¹⁴ These results demonstrate substantial agreement between readers using the same grading scheme for ultrawide field images. This level of agreement is equivalent to previously reported levels of agreement in large multicenter clinical trials using a centralized reading center.^{4,11–13}

Mydriatic Ultrawide Field Agreement with Early Treatment Diabetic Retinopathy Study Film Photographs and Dilated Fundus Examination

The severity of DR identified on DiSLO200 images agreed exactly with ETDRS film photographs in 80% of eyes and was within 1 step in 94.5% of eyes ($\kappa = 0.74$ [95% CI, 0.67–0.81], weighted

Table 1. Study Participant Characteristics

Baseline Patient Demographics (N=103 Patients)	Mean \pm Standard Deviation (Range) or N (%)
Age (yrs)	53.9 \pm 15.2 (18–88)
Female/male	51 (49.5%)/52 (50.5%)
Race	
White	83 (80.6%)
African-American	9 (8.7%)
Hispanic	3 (2.9%)
Asian	1 (1.0%)
Other/Unspecified	7 (6.8%)
Ocular Characteristics (N = 206 Eyes)	
ETDRS Electronic Visual Acuity (Letter Score/Snellen Equivalent)	
Median	85 (20/20)
Range	35 to 98 (20/200–20/12.5)
$\geq 20/20$	145 (70.4%)
$< 20/20$ to $\geq 20/40$	50 (24.3%)
$< 20/40$ to $\geq 20/100$	10 (4.9%)
$< 20/100$	1 (0.5%)
Retinopathy Severity*	
No DR	25 (12.5%)
Mild NPDR	45 (22.5%)
Moderate NPDR	60 (30.0%)
Severe NPDR	13 (6.5%)
Very severe NPDR	3 (1.5%)
PDR	46 (23.0%)
High-risk PDR	8 (4.0%)
Ungradable	0 (0.0%)
Macular Edema Severity*	
No DME	115 (57.5%)
DME	35 (17.5%)
CSME	41 (20.5%)
Ungradable for DME	9 (4.5%)

CSME = clinically significant macular edema; DME = diabetic macular edema; DR = diabetic retinopathy; ETDRS = Early Treatment Diabetic Retinopathy Study; NPDR = nonproliferative diabetic retinopathy; PDR = proliferative diabetic retinopathy.

*Grading based on ETDRS 35-mm 7-standard film photographs. Six eyes did not complete imaging (N = 200 eyes).

$\kappa = 0.84$ [95% CI, 0.79–0.89]) (Table 2). When DiSLO200 did not match photographs (N = 40 eyes), DiSLO200 was deemed more accurate in 57.5% of eyes (23) on the basis of direct side-by-side comparison with ETDRS film photographs. Compared with dilated fundus examinations, there was exact agreement with the level of DR identified on DiSLO200 images in 58.8% of eyes and agreement was within 1 step in 91.2% of eyes ($\kappa = 0.47$ [95% CI, 0.39–0.56], weighted $\kappa = 0.69$ [95% CI, 0.62–0.76]) (Table 3).

Discrepancies in Diabetic Retinopathy Severity between Mydriatic Ultrawide Field Images and Early Treatment Diabetic Retinopathy Study Film Photographs

The senior retinal specialist performed side-by-side adjudication of all eyes that had DR severity discrepancies between ETDRS film photographs and DiSLO200 imaging, noting the underlying cause of the discrepancy and explanation (grader error, image quality, or field coverage). On the basis of the side-by-side comparison, the senior retinal specialist selected the imaging modality that was believed to demonstrate DR severity more accurately on the basis of image quality and presence and extent of retinal lesions identified. Appropriate statistical evaluation of these data was not

Table 2. Cross Tabulation of Number of Eyes with Level of Diabetic Retinopathy Derived from Mydriatic 200-Degree Ultrawide Field Images and 35-mm ETDRS Film Photographs

Grading by 35-mm ETDRS Film Photographs	Grading by Mydriatic Ultrawide Field 200-Degree Images								Total (%)
	DR Absent	Mild NPDR	Moderate NPDR	Severe NPDR	Very Severe NPDR	PDR Less Than High Risk	High-Risk PDR	Ungradable	
DR absent	17	7	1	0	0	0	0	0	25 (12.5)
Mild NPDR	3	30	11	1	0	0	0	0	45 (22.5)
Moderate NPDR	0	2	55	2	0	1	0	0	60 (30)
Severe NPDR	0	1	4	7	0	1	0	0	13 (6.5)
Very severe NPDR	0	0	0	0	3	0	0	0	3 (1.5)
PDR less than high risk	0	1	3	2	0	40	0	0	46 (23)
High-risk PDR	0	0	0	0	0	0	8	0	8 (4)
Ungradable	0	0	0	0	0	0	0	0	0 (0)
Total (%)	20 (10)	41 (20.5)	74 (37)	12 (6)	3 (1.5)	42 (21)	8 (4.0)	0 (0)	200

CI = confidence interval; DR = diabetic retinopathy; ETDRS = Early Treatment Diabetic Retinopathy Study; NPDR = nonproliferative diabetic retinopathy; PDR = proliferative diabetic retinopathy. Perfect agreement: 80.0%; within 1-step agreement: 94.5%. Simple kappa statistic: 0.74 (95% CI, 0.67–0.81); weighted kappa statistic (linear scale): 0.84 (95% CI, 0.79–0.89).

possible because of the small subset of the images that required comparison (N = 40).

In the 40 eyes (20%) that had discrepancies in DR severity between DiSLO200 images and ETDRS film photographs after adjudication and side-by-side comparison, DiSLO200 images were selected as the potentially more accurate modality in 57% (23 eyes) and ETDRS film photographs in 43% (17 eyes).

The retinal lesions (46 lesions in 40 eyes) causing discrepancies in DR severity (3 lesion types in 1 eye, 2 types in 4 eyes, and a single type in 35 eyes) were H/Ma in 52% (24 lesions in 22 eyes), IRMA in 26% (12 lesions in 8 eyes), NVE in 17% (8 lesions in 8 eyes), and VB in 4% (2 lesions in 2 eyes). DiSLO200 images were evaluated to be more accurate (N = 23, 57% of eyes with discrepancy, 11.5% of total eyes) in 3 eyes (7.5% of eyes with discrepancy, 1.5% of total eyes) because of inadequate ETDRS film photograph quality and in 20 eyes (50% of eyes with discrepancy and 10% of total eyes) because the lesions were located outside ETDRS film photograph fields.

When DiSLO200 images were deemed the more accurate modality, the differences in identifying DR lesions led to

DiSLO200 images suggesting a 1-step change in DR severity in 23 eyes. Among these, 22 eyes (11.0% of total eyes) would have had more severe DR and 1 eye (0.5%) would have less severe DR. A 2-step or greater worsening would have occurred in 3 eyes (1.5%). New vessels elsewhere were observed by DiSLO200 and not observed with ETDRS film photographs in 2 eyes (1%).

In eyes in which ETDRS film photographs were judged to be the more accurate imaging modality (N = 17, 8.5% of total eyes), inadequate DiSLO200 image quality was the cause in all cases. These discrepancies led to ETDRS film photographs providing a 1-step change in DR severity in 10 eyes, with more severe DR in 8 eyes (4%) and less severe DR in 2 eyes (1%). A 2-step or greater worsening occurred in 7 eyes (3.5%), and PDR that was not observed by DiSLO200 imaging was noted in 6 eyes (3%). On DiSLO200 imaging, these 6 eyes with PDR were graded as mild nonproliferative DR (NPDR) in 1 eye, moderate NPDR in 3 eyes, and severe NPDR in 2 eyes. In all 6 eyes, PDR was not documented on clinical examination (1 eye reported as mild NPDR, 4 eyes reported as moderate NPDR, 1 eye reported as severe NPDR).

Table 3. Cross Tabulation of Number of Eyes with Level of Diabetic Retinopathy Derived from Mydriatic 200-Degree Ultrawide Field Images and Dilated Fundus Examination

Grading by Dilated Fundus Examination	Grading by Mydriatic Ultrawide Field 200-Degree Images								Total (%)
	DR Absent	Mild NPDR	Moderate NPDR	Severe NPDR	Very Severe NPDR	PDR Less than High Risk	High-Risk PDR	Ungradable	
DR absent	16	11	1	0	0	1	0	0	29 (14.1)
Mild NPDR	4	23	19	0	0	0	0	2	48 (23.3)
Moderate NPDR	0	4	44	8	1	5	0	0	62 (30.1)
Severe NPDR	0	1	9	6	2	4	0	0	22 (10.7)
Very severe NPDR	0	0	0	0	0	1	0	0	1 (0.5%)
PDR less than high risk	0	2	3	0	0	28	5	0	38 (18.4%)
High-risk PDR	0	0	0	0	0	3	3	0	6 (2.9%)
Ungradable	0	0	0	0	0	0	0	0	0 (0%)
Total (%)	20 (9.7)	41 (19.9)	76 (36.9)	14 (6.8)	3 (1.5)	42 (20.4)	8 (3.9)	2 (1)	206

CI = confidence interval; DR = diabetic retinopathy; NPDR = nonproliferative diabetic retinopathy; PDR = proliferative diabetic retinopathy. The following measures did not include images that were ungradable by ultrawide field imaging and dilated fundus examination, N (included) = 204. Perfect agreement: 58.8%; within 1-step agreement: 91.2%. Simple kappa statistic: 0.47 (95% CI, 0.39–0.56); weighted kappa statistic (linear scale): 0.69 (95% CI, 0.62–0.76).

Identification of Diabetic Retinopathy Lesions

Table 4 (available at <http://aaojournal.org>) presents a detailed assessment of the identification and severity of individual DR lesions comparing the DiSLO200 images and ETDRS film photographs. At the lesion level, there was substantial agreement between DiSLO200 images and ETDRS film photographs for H/Ma, IRMA, and NVE. There was moderate agreement for VB and NVE. Overall, DiSLO200 imaging identified key DR lesions as accurately as ETDRS film photographs in 92% of NVD, 96.5% of NVE, 86% of VB, 82% of IRMA, and 78% of H/Ma cases.

Considering only fields that were gradable by both modalities for the specific DR lesion, DiSLO200 imaging suggested a more severe DR level in 15% of H/Ma, 10% of VB, 12% of IRMA, and 2.9% of NVE cases. The ETDRS film photographs identified a more severe DR level in 7% of H/Ma, 4% of VB, 6% of IRMA, and 0.6% of NVE cases (Table 5, available at <http://aaojournal.org>).

Distribution of Diabetic Retinopathy Lesions

More than 60% of all DR lesions are predominantly evident in the retinal area imaged by ETDRS defined fields (Fig 2). However, approximately one-third of H/Ma, IRMA, and NVE were located predominantly outside the ETDRS defined 7-standard fields. These peripheral lesions located outside the ETDRS 7-standard fields suggested a more severe assessment of DR in 20 eyes (10%). Among these 20 eyes, discrepancies would have resulted in severity changes from no DR to mild NPDR in 5 eyes, mild NPDR to moderate NPDR in 10 eyes, no DR to moderate NPDR in 1 eye, mild NPDR to severe NPDR in 1 eye, moderate NPDR to severe NPDR in 1 eye, moderate NPDR to PDR in 1 eye, and severe NPDR to PDR in 1 eye.

DiSLO200 images demonstrated a nonuniform retinal distribution of DR lesions (Fig 3). Venous beading, H/Ma, IRMA, and NVE were more prevalent in the temporal fields than in the nasal fields ($P < 0.0001$, all 4 lesions). By excluding fields that were ungradable, H/Ma was found in 81% of temporal, 76% of superotemporal, 67% of superonasal, 67% of inferotemporal, and 68% of inferonasal fields. A similar distribution trend was observed for IRMA and to a lesser extent for NVE (Fig 4, available at <http://aaojournal.org>).

Effect of Mydriasis on Ungradable Rate and Agreement with Early Treatment Diabetic Retinopathy Study Film Photographs

Mydriatic ultrawide field imaging did not result in a statistically significant increase in the overall agreement with ETDRS film photographs compared with nonmydriatic ultrawide field imaging performed at the same time and read previously as published in another study (Fig 5).¹⁴ However, pharmacologic mydriasis reduced the ungradable rate of ultrawide field images from 4.5% (9 eyes) to 0% ($P = 0.002$). Mydriatic DiSLO200 imaging generally improved the individual lesion agreement for H/Ma, VB, IRMA, and NVE with ETDRS film photographs compared with nonmydriatic Optos imaging as shown in Figure 6 (available at <http://aaojournal.org>). DiSLO200 image ungradable rates for peripheral lesions were 2-fold greater in the inferior temporal field and 3-fold greater in the inferior nasal field compared with the temporal, superior temporal, and superior nasal fields (Fig 7, available at <http://aaojournal.org>).

Discussion

Mydriatic ultrawide field imaging demonstrated substantial agreement with ETDRS film photographs and DFE in

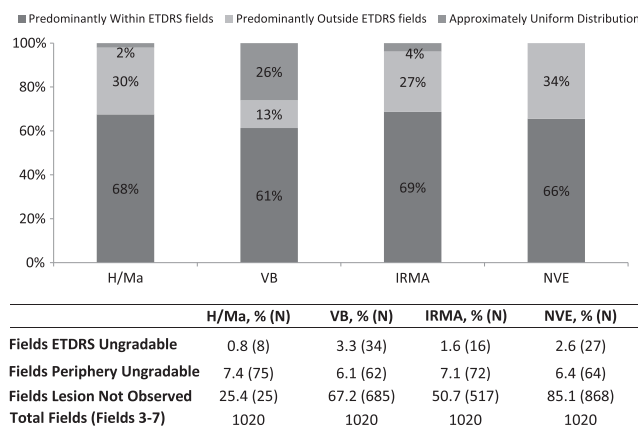
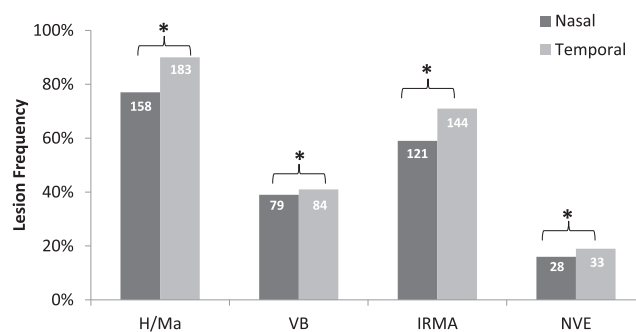


Figure 2. Distribution of diabetic retinopathy (DR) lesions identified on mydriatic 200-degree ultrawide field images. ETDRS = Early Treatment Diabetic Retinopathy Study; H/Ma = hemorrhage and/or microaneurysm; IRMA = intraretinal microvascular abnormality; NVE = new vessels elsewhere; VB = venous beading.

determining DR severity, with 94.5% of eyes within 1 step of agreement. Compared with nonmydriatic ultrawide field imaging, mydriasis reduced the ungradable rate from 4.5% to 0% with a statistically nonsignificant increase in agreement. When DiSLO200 images did not match ETDRS film photographs, DiSLO200 images were deemed more accurate in 57% of eyes after side-by-side image comparison.

One of the key features of ultrawide field imaging is the additional retinal surface area that can be examined (~30% of the retinal area for all 7 fields with ETDRS film photographs compared with ~82% for the ultrawide 200-degree field). In addition, ultrawide field imaging provides a single contiguous area for evaluation. In this cohort of patients selected to encompass the full spectrum of clinical DR severity, approximately one-third of H/Ma, IRMA, and NVE lesions were located outside the retinal area imaged by ETDRS 7 fields but were visible using ultrawide field imaging. Lesions observed outside of the ETDRS 7-standard fields would have suggested a more severe grade of DR in 10% of eyes. However, the implications of these peripheral lesions on DR progression are unknown and need to be evaluated in a prospective manner.



*p value <0.0001

Figure 3. Comparison of diabetic retinopathy (DR) lesion frequency in temporal and nasal retinal fields. H/Ma = hemorrhage and/or microaneurysm; IRMA = intraretinal microvascular abnormality; NVE = new vessels elsewhere; VB = venous beading.

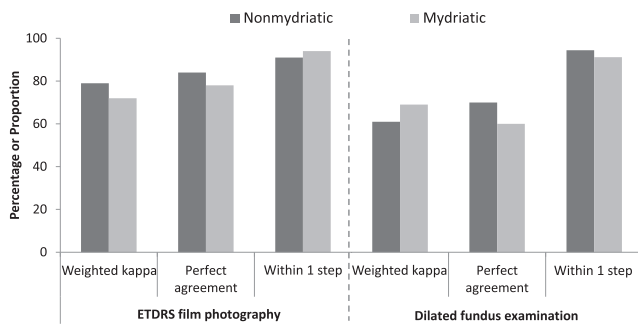


Figure 5. Agreement of nonmydriatic and mydriatic 200-degree ultrawide field imaging with Early Treatment Diabetic Retinopathy Study (ETDRS) film photography and dilated fundus examination to identify severity of diabetic retinopathy (DR).

The identification of lesions by ultrawide field imaging in areas not imaged by ETDRS film photographs suggests that this information might be useful in determining more accurately the specific risk of DR progression in an individual patient than possible with ETDRS film photographs alone. Previous studies have suggested that some of the earliest clinical changes in DR may occur in the midperipheral fundus.^{19,20} Although 10% of eyes might have been classified with more severe retinopathy when assessing these additional lesions, it is not known whether the extent of additional peripheral lesions (whether or not they resulted in an increase in presumed DR severity grade) places a patient at increased risk of retinopathy progression. In this case, more overall lesions in the retina might be associated with a greater risk of retinopathy progression and complications even though a patient might have the same general ETDRS DR severity level. Conversely, it is not known whether these additional lesions actually add to the determination of risk that can already be obtained from ETDRS film photographs, which are good predictors of DR severity and progression.⁴ These peripheral lesions were presumably present (even if unable to be imaged) when the ETDRS photographic risk assessments were made, and thus they were incorporated to some degree already in the ETDRS progression risk profiles. However, it is possible that identification of midperipheral and peripheral changes may be associated with increased risk of DR progression, although determination of this association and its clinical relevance will necessitate future prospective trials evaluating a broad range of DR severity across a diversity of diabetic patient populations.

The sensitivity and specificity for identifying posterior DR lesions with nonmydriatic ultrawide field imaging have been shown to be comparable to retinal photography and clinical examination.^{14–16} In this study of patients without substantial media opacity, we find that mydriasis reduces the ultrawide field imaging ungradable image rate from 4.5% to 0%. The majority of DR severity discrepancies between DiSLO200 images and ETDRS film photographs was attributable to H/Ma (22 eyes; 52%). In 17 of these 22 eyes (77.2%), DiSLO200 images were judged to be more accurate than ETDRS film photographs, suggesting a classification of more severe DR.

The nonuniform retinal distribution of DR lesions has been reported on the basis of experimental work in

galactosemic dogs²¹ and human autopsy specimens.²² Our results in a diverse patient population using in vivo high-resolution ultrawide field imaging are consistent with these reports and demonstrate peripheral pathology primarily in the temporal and superior quadrants. Clinically, retinal neovascularization occurs most frequently in the superior temporal quadrant (Prud'homme G, Rand L. The Diabetic Retinopathy Study Research Group: Distribution of maximum grade of lesion in proliferative diabetic retinopathy. Presented at: ARVO Annual Spring Meeting, April 26 to May 1, 1981, Sarasota, FL).²³ Similar regional differences across the retina in retinal oxygenation and blood flow also have been reported.^{24,25} The clinical implication of this nonuniform distribution of DR lesions is uncertain but may imply predisposition or protection of certain areas to diabetes-induced retinal changes.

Wide-field 130-degree fluorescein angiographic studies describe 4 distinct patterns of retinal capillary nonperfusion in eyes with NPDR: (1) peripheral, (2) midperipheral, (3) central, and (4) generalized.²⁰ The most common pattern was midperipheral nonperfusion defined as nonperfusion within 6 disc diameters from the optic disc without involving the central retina and optic disc. This observation has commonly been cited as the rationale behind midperipheral development of NPDR changes.^{19,20} The site of nonperfusion was shown to correlate closely with progression to PDR in patients with NPDR over a period of 2 to 42 months (mean, 11.6 months). Thus, it is possible that identification of midperipheral and peripheral changes in particular quadrants may be associated with increased risk of DR progression, although determination of this association and its clinical relevance will necessitate future prospective trials.

Current ultrawide field imaging technology provides good image resolution and detail across a horizontal band covering the disc and macula, and extending peripherally past the equator. Fine retinal vascular lesions extending to the temporal and nasal periphery are readily observed within this area, encompassing ETDRS fields 1, 2, and 3. However, because of spherical aberrations, different focus distances, and the natural curvature of the globe, the retinal areas imaged anterior to the superior and inferior vascular arcade exhibit modest blurring and may lack adequate detail to evaluate fine retinal vascular lesions in these areas, such as a subtle NVE or IRMA. In addition, the patient's eyelids and eyelashes may cause artifacts that can partially obscure the superior and inferior retinal fields. Indeed, in the 16 eyes in which IRMA or NVE primarily caused the discrepancy, ETDRS film photographs were judged the more accurate modality in 12 (75%) because of inadequate DiSLO200 image quality. This local clarity issue is present despite the use of pharmacologic mydriasis and is reflected in the 2- to 3-fold greater ungradable rates in the inferior retinal fields. In addition, on the basis of the imaging protocol used in this study, at least two 200-degree images (stereoscopic pair) were taken for each eye that may have contributed to a lower rate of ungradable images.

In conclusion, although ETDRS film photography or its digital equivalent remains the gold standard for evaluating DR, clinicians often consider peripheral and midperipheral findings in identifying the presence and assessing

the severity of DR. In DR, ultrawide field fluorescein angiography has been shown to reveal approximately 4 times more retinal nonperfusion and approximately 2 times more NVE than fluorescein angiography using the ETDRS 7-standard 30-degree fields.²⁶ Our data demonstrate that ultrawide field imaging identifies substantially more diabetic retinal vascular pathology even without the use of fluorescein angiography. Data from prospective studies will be needed to establish the clinical role and impact on risk assessment of the additional lesion detection derived from ultrawide field imaging.

References

1. Diabetic Retinopathy Study Research Group. Photocoagulation treatment of proliferative diabetic retinopathy. Clinical application of Diabetic Retinopathy Study (DRS) findings, DRS report number 8. *Ophthalmology* 1981;88:583–600.
2. Early Treatment Diabetic Retinopathy Study Research Group. Treatment techniques and clinical guidelines for photocoagulation of diabetic macular edema. Early Treatment Diabetic Retinopathy Study Report Number 2. *Ophthalmology* 1987;94:761–74.
3. Early Treatment Diabetic Retinopathy Study Research Group. Early photocoagulation for diabetic retinopathy. ETDRS report number 9. *Ophthalmology* 1991;98:766–85.
4. Early Treatment Diabetic Retinopathy Study Research Group. Fundus photographic risk factors for progression of diabetic retinopathy. ETDRS report number 12. *Ophthalmology* 1991;98:823–33.
5. Diabetic Retinopathy Vitrectomy Study Research Group. Early vitrectomy for severe proliferative diabetic retinopathy in eyes with useful vision. Clinical application of results of a randomized trial—Diabetic Retinopathy Vitrectomy Study report 4. *Ophthalmology* 1988;95:1321–34.
6. Diabetes Control and Complications Trial Research Group. The effect of intensive treatment of diabetes on the development and progression of long-term complications in insulin-dependent diabetes mellitus. *N Engl J Med* 1993;329:977–86.
7. Writing Team for the Diabetes Control and Complications Trial/Epidemiology of Diabetes Interventions and Complications (EDIC) Study Research Group. Sustained effect of intensive treatment of type 1 diabetes mellitus on development and progression of diabetic nephropathy: the Epidemiology of Diabetes Interventions and Complications (EDIC) Study. *JAMA* 2003;290:2159–67.
8. UK Prospective Diabetes Study (UKPDS) Group. Intensive blood-glucose control with sulphonylureas or insulin compared with conventional treatment and risk of complications in patients with type 2 diabetes (UKPDS 33). *Lancet* 1998;352:837–53.
9. Holman RR, Paul SK, Bethel MA, et al. 10-year follow-up of intensive glucose control in type 2 diabetes. *N Engl J Med* 2008;359:1577–89.
10. Diabetic Retinopathy Clinical Research Network, Elman MJ, Aiello LP, Beck RW, et al. Randomized trial evaluating ranibizumab plus prompt or deferred laser or triamcinolone plus prompt laser for diabetic macular edema. *Ophthalmology* 2010;117:1064–77.
11. Gangaputra S, Almutkhar T, Glassman AR, et al; Diabetic Retinopathy Clinical Research Network. Comparison of film and digital fundus photographs in eyes of individuals with diabetes mellitus. *Invest Ophthalmol Vis Sci* 2011;52:6168–73.
12. Hubbard LD, Sun W, Cleary PA, et al; Diabetes Control and Complications Trial/Epidemiology of Diabetes Interventions and Complications Study Research Group. Comparison of digital and film grading of diabetic retinopathy severity in the Diabetes Control and Complications Trial/Epidemiology of Diabetes Interventions and Complications Study. *Arch Ophthalmol* 2011;129:718–26.
13. Li HK, Danis RP, Hubbard LD, et al. Comparability of digital photography to the ETDRS film protocol for evaluation of diabetic retinopathy severity. *Invest Ophthalmol Vis Sci* 2011;52:4717–25.
14. Silva PS, Cavallerano JD, Sun JK, et al. Nonmydriatic ultrawide field retinal imaging compared with dilated standard 7-field 35-mm photography and retinal specialist examination for evaluation of diabetic retinopathy. *Am J Ophthalmol* 2012;154:549–59.
15. Wilson PJ, Ellis JD, MacEwen CJ, et al. Screening for diabetic retinopathy: a comparative trial of photography and scanning laser ophthalmoscopy. *Ophthalmologica* 2010;224:251–7.
16. Mackenzie PJ, Russell M, Ma PE, et al. Sensitivity and specificity of the Optos Optomap for detecting peripheral retinal lesions. *Retina* 2007;27:1119–24.
17. Landis JR, Koch GG. The measurement of observer agreement for categorical data. *Biometrics* 1977;33:159–74.
18. Early Treatment Diabetic Retinopathy Study Research Group. Grading diabetic retinopathy from stereoscopic color fundus photographs—an extension of the modified Airlie House classification. ETDRS report number 10. *Ophthalmology* 1991;98(Suppl):786–806.
19. Shimizu K, Kobayashi Y, Muraoka K. Midperipheral fundus involvement in diabetic retinopathy. *Ophthalmology* 1981;88:601–12.
20. Niki T, Muraoka K, Shimizu K. Distribution of capillary nonperfusion in early-stage diabetic retinopathy. *Ophthalmology* 1984;91:1431–9.
21. Kern TS, Engerman RL. Vascular lesions in diabetes are distributed non-uniformly within the retina. *Exp Eye Res* 1995;60:545–9.
22. Tang J, Mohr S, Du YD, Kern TS. Non-uniform distribution of lesions and biochemical abnormalities within the retina of diabetic humans. *Curr Eye Res* 2003;27:7–13.
23. Taylor E, Dobree JH. Proliferative diabetic retinopathy: site and size of initial lesions. *Br J Ophthalmol* 1970;54:11–8.
24. Berkowitz BA, Kowluru RA, Frank RN, et al. Subnormal retinal oxygenation response precedes diabetic-like retinopathy. *Invest Ophthalmol Vis Sci* 1999;40:2100–5.
25. Schwartz B, Harris A, Takamoto T, et al. Regional differences in optic disc and retinal circulation. *Acta Ophthalmol Scand* 2000;78:627–31.
26. Wessel MM, Aaker GD, Parlitsis G, et al. Ultra-wide-field angiography improves the detection and classification of diabetic retinopathy. *Retina* 2012;32:785–91.

Footnotes and Financial Disclosures

Originally received: January 14, 2013.
Final revision: April 25, 2013.

Accepted: May 2, 2013.
Available online: June 17, 2013.

Manuscript no. 2013-76.

¹ Beetham Eye Institute, Joslin Diabetes Center, Boston, Massachusetts.

² Department of Ophthalmology, Harvard Medical School, Boston, Massachusetts.

Presented at: the American Academy of Ophthalmology Annual Meeting, November 10–13, 2012, Chicago, Illinois.

Financial Disclosure(s):

The Joslin Diabetes Center received a temporary equipment loan and unrestricted research grant funding for the performance of initial validation studies on the Optos, plc, ultrawide field retinal imager from Optos, plc (Dunfermline, Fife, Scotland, UK). No additional outside funding was received for the performance of the research presented in this report.

Funding:

The performance of the study published by Silva et al¹⁴ was supported in part by grant funding provided to the Joslin Diabetes Center by Optos, plc,

(Dunfermline, Fife, Scotland, UK). Ultrawide field images taken during that study were acquired on an Optos P200MA that was provided by Optos, plc, to the Joslin Diabetes Center on temporary loan. Subsequent studies that reviewed images obtained from the original cohort of patients reported in this article received no external funding. Optos, plc, was the partial sponsor and funding organization of the initial study and had no oversight in the design, conduct, or reports of the past or current research.

Correspondence:

Paolo S. Silva, MD, Beetham Eye Institute, Joslin Diabetes Center, One Joslin Place, Boston, MA 02215. E-mail: paoloantonio.silva@joslin.harvard.edu.